



## **Geopolymer Bio-Patch Repair: Microbially-Induced Calcite and Pozzolanic Fly Ash and Rice Husk Ash for Corrosion-Resistant of Reinforced Concrete Repair**

**Pinta Astuti<sup>1\*</sup>, Angga Jordi Wisnu Nouvaldi<sup>1</sup>, Aprilia Rahmayanti<sup>1</sup>, Pramudya Surya Shabura<sup>1</sup>, Muhammad Etandra Fara Adzani<sup>1</sup>, Dylan Ataa Tsany<sup>1</sup>, Adhitya Yoga Purnama<sup>2</sup>, Rahmita Sari Rafdinal<sup>3</sup>**

<sup>1</sup>Department of Civil Engineering, Faculty of Engineering, Universitas Muhammadiyah Yogyakarta, Jalan Brawijaya, Tamantirto, Kasihan, Bantul, 55183, Daerah Istimewa Yogyakarta, Indonesia

<sup>2</sup>Department of Civil Engineering, Vocational College, Universitas Gadjah Mada, Jalan Yacaranda, Blimbingsari, Caturtunggal, Depok, Sleman, 55281, Daerah Istimewa Yogyakarta, Indonesia

<sup>3</sup>Limited Area Manager, PS. Construction Co. Ltd., 8F Tokyo Shiodome Bldg., 1-9-1, Higashi Shimbashi, Minato-ku, 105-7365, Tokyo, Japan

\*[pinta.astuti@ft.umy.ac.id](mailto:pinta.astuti@ft.umy.ac.id)

**Abstract.** Indonesia's archipelagic environment subjects concrete structures to severe corrosion and sulfate attacks, necessitating sustainable repair solutions. This study evaluates a geopolymer-based bio-patch repair mortar utilizing fly ash (FA), rice husk ash (RHA), and *Bacillus subtilis* bacteria to induce Microbially Induced Calcite Precipitation (MICP). While the silica-rich ashes act as pozzolanic materials, the bacteria enhance durability by reducing oxygen levels and lowering corrosion rates. Microscopic analysis confirmed the formation of calcium carbonate ( $\text{CaCO}_3$ ) and calcium silicate hydrate (C-S-H), both of which significantly improve mechanical properties. The research identified an optimum mixture of 93% FA, 6% RHA, and 1% bacteria, which achieved a compressive strength of 30 MPa, a density of 2.32 g/cm<sup>3</sup>, and a low water absorption rate of 3.25%. These results meet standard performance requirements, demonstrating that this eco-friendly geopolymer-MICP system is a viable and innovative contribution to structural repair in aggressive environments.

**Keywords:** corrosion protection, fly ash, geopolymer mortar, microbially induced calcite precipitation (MICP), rice husk ash

*(Received 2025-09-14, Revised 2026-11-17, Accepted 2026-01-29, Available Online by 2026-01-31)*

## 1. Introduction

Indonesia is an archipelago, so some of its territory is directly connected to the sea. These conditions are corrosive environmental conditions and prone to corrosion attacks on building structures [1]. In aggressive environments, concrete and mortar will be exposed to sulfates and high acidity, making concrete and mortar susceptible to damage in the form of cracks [2–5]. Cracks occur due to the volume of rust in the corroded reinforcing steel being greater than  $\pm 3$  times the volume of the original material. If allowed to continue, the width of the cracks will increase and the number of cracks will increase, resulting in a decrease in strength and can shorten the service life of the construction [6,7].

A common method used to overcome these challenges is conventional cement-based patch repair. The patch repair method is a technique to repair old structures by restoring their original shape and strength [8–10]. However, the use of conventional cement has limitations in protecting concrete from corrosion in the long term under extreme environmental conditions such as in Indonesia. Conventional cements tend to be ineffective in resisting seawater penetration and protection against corrosion induced by acidic and sulfuric environments [11–15]. The development of sustainable construction materials is also becoming increasingly important in reducing environmental impacts and improving infrastructure resilience. Geopolymer mortars are mortars with binders using natural materials containing oxides of silica and high alumina, activated with alkali activators such as sodium hydroxide (NaOH) and sodium silicate ( $\text{Na}_2\text{SiO}_3$ ) as catalysts to accelerate the polymerization reaction [16–18]. It has attracted attention as a viable alternative to conventional cement due to its lower carbon footprint and superior durability [19–21]. It offers a promising solution to repair and enhance the durability of concrete structures, especially when complemented with complementary materials and innovative approaches such as microbial agents [22,23].

In this research, a combination of *Bacillus subtilis* bacteria and rice husk ash was used as an inhibitor in the bio-patch repair method for corrosion protection of reinforced concrete. Studies on the utilization of *Bacillus subtilis* bacteria and rice husk ash as bio-patch repair are based on the properties of these materials. Research by previous study showed that *Bacillus subtilis* bacteria in the aerobic metabolic process can reduce the concentration of dissolved oxygen so that it can reduce the corrosion rate of metals [24,25]. *Bacillus subtilis* bacteria are also used as a medium to repair cracks in concrete and mortar. Different concentrations of bacteria in concrete will affect the durability of concrete [26–30]. Meanwhile, rice husk ash has a fairly high silica content, which is around 87-97% from the combustion process. The high silica content in rice husk ash can be used as an inhibitor to control corrosion of reinforcing steel [30–33].

Rice husk ash, a by-product of rice milling, presents significant environmental disposal challenges. However, rice husk ash is rich in silica that can react with calcium hydroxide to form additional calcium silicate hydrate (C-S-H), thereby improving mechanical properties and durability [34–36]. The utilization of rice husk ash not only addresses waste management issues but also contributes to the development of environmentally friendly construction materials. Another innovative approach to improve concrete performance is through microbial induced calcite precipitation (MICP) [37]. MICP is a process in which bacteria, such as *Bacillus subtilis*, facilitate the formation of calcium carbonate (calcite) in the concrete matrix [38]. This biominerization process can effectively fill cracks and pores, thereby improving the impermeability and mechanical strength of concrete [26,37,38]. The application of MICP in repair mortars presents a promising solution for sustainable and durable concrete repair.

So as a research development effort, further research will be conducted in examining the combined utilization of rice husk ash and *Bacillus subtilis* bacteria as a bio-patch repair mortar for corrosion protection of concrete due to no previous research reported the use of geopolymer using biodegradable material and bacteria as a patching material that presented the viability of *Bacillus subtilis* bacteria in alkaline geopolymer matrix patch repair. The synergistic mechanism interaction between fly ash, rice husk ash, and the microbially induced calcite precipitation (MICP) is observed. The pozzolanic activity of rice husk ash, combined with calcite precipitation induced by *Bacillus subtilis* could be a potential for better crack sealing, improved mechanical properties, and enhanced resistance to environmental degradation. This innovative approach not only addresses the immediate repair needs but also

contributes to the long-term durability and sustainability of concrete structures. Through this approach, it is hoped that an environmentally friendly and effective repair method can be developed to extend the service life of concrete structures and reduce the impact of corrosion.

## 2. Methods

### 2.1. Materials

The materials used in this research consist of fine aggregate, fly ash, rice husk ash, and *Bacillus subtilis* bacteria. Fine aggregate, in accordance with SNI S-04-1989-F, is defined as particles that pass through a 4.75 mm sieve, and in this study, it was obtained from Kulon Progo. Fly ash, a by-product of coal combustion in power plants, contains pozzolanic fine particles rich in silica and alumina. The fly ash used in this research was sourced from PT Varia Usaha Beton. Rice husk ash, derived from the milling of rice and subsequent burning of the husk, was incorporated due to its high silica content, making it suitable as a cement substitute. Meanwhile, *Bacillus subtilis* bacteria, cultivated at the Agrobiotechnology Laboratory, Faculty of Agriculture, Universitas Muhammadiyah Yogyakarta, were utilized as a biological self-healing agent to enhance the performance of the material system. *Bacillus subtilis* spores were prepared and immobilized prior to incorporation into the mixture. The bacterial culture was first grown in nutrient broth at 30 °C for 24 h until reaching the late-exponential phase, followed by induction of sporulation using a nutrient-depletion method. The spores were harvested by centrifugation (4000 rpm, 10 min), washed twice with sterile distilled water, and subsequently immobilized in calcium-lactate powder as a protective carrier. The final culture density used in this study was approximately  $1 \times 10^7$ – $10^8$  CFU/mL, which is commonly reported as adequate for self-healing applications. To prevent cell inactivation during mixing with the highly alkaline activator, only dried and encapsulated spores were added to the binder system, ensuring that viable cells were not directly exposed to the fresh alkaline environment. The spores were activated only after microcrack formation allowed moisture ingress, enabling germination under more favorable pH conditions.

### 2.2. Materials characteristic

The testing of materials in this research included fine aggregate, rice husk ash, and *Bacillus subtilis* bacteria. Fine aggregate testing followed SNI standards and consisted of several stages: the specific gravity test (SNI 1970:2016) to determine bulk, dry, and apparent specific gravity using a graduated flask; the fineness modulus test (SNI ASTM C136-2012) through sieve analysis and percentage weight calculation; the water content test (SNI 1971:2011) by comparing mass before and after oven drying; and the mud content test (SK SNI S-04-1989 F) by comparing mass before and after washing the aggregates. Rice husk ash testing involved three methods: the specific gravity test (ASTM C188-89) using a 500 ml volumetric flask to calculate mass-to-volume ratio; Fourier Transform Infrared Spectroscopy (FTIR) to identify functional chemical groups based on infrared absorption; and X-Ray Fluorescence (XRF) to determine elemental composition through energy spectrum analysis of fluorescent X-rays. Meanwhile, *Bacillus subtilis* bacteria were subjected to morphological identification and characterization through cell shape observation, Gram staining to confirm Gram-positive nature, and endospore detection, in accordance with literature. These tests were conducted at the Agrobiotechnology Laboratory, Faculty of Agriculture, Universitas Muhammadiyah Yogyakarta.

### 2.3. Experimental procedures

The experimental procedure consisted of the preparation of test specimens, evaluation of fresh and hardened properties, patch repair testing, and self-healing assessment. Test specimens were prepared in the form of paste, mortar cubes (5 × 5 × 5 cm), self-healing prisms (16 × 5 × 5 cm), and bio-patch repair blocks (40 × 15 × 15 cm). The geopolymers paste composition was prepared in accordance with SNI-03-6827-16 2002 using the Vicat test method. The curing regime followed a standard procedure for low-calcium geopolymers binders, which require controlled thermal activation to accelerate polycondensation. Specifically, all specimens were initially cured in an oven at 70 °C for 24 hours,

allowing the dissolution of aluminosilicate precursors and the formation of N-A-S-H gel. After thermal curing, specimens were removed from the oven, allowed to cool to room temperature, sealed with aluminum foil, and stored under sealed-curing conditions up to 28 days to prevent moisture loss and carbonation, both of which may disrupt geopolymers. This sealed-curing approach is widely recommended for geopolymers because maintaining internal moisture is essential for continued reaction and strength development. For the bio-patch repair specimens, the blocks were prepared through mix design, casting, and curing following the same regime. To simulate deteriorated conditions, 10 kg/m<sup>3</sup> of salt was incorporated during initial casting. At 21 days, the specimens were re-cast to complete the bio-patch repair system while ensuring minimal disturbance to the partially cured matrix.

The fresh properties of mortar were assessed by the flow table test (SNI 6882-2014), in which the average spread diameter was measured to ensure flow values of 105–115%. Density was determined according to SNI 1973-2016 by dividing the mortar mass by the known mold volume. Hardened properties were evaluated through compressive strength, shrinkage, absorption, microstructural analysis, and setting time tests. Compressive strength was measured using a compression testing machine following SNI 03-6825-2002 at curing ages of 7, 14, and 28 days. Shrinkage was determined by measuring dimensional changes before and after curing, while water absorption was tested in accordance with ASTM C-1403-15 at intervals of 15 minutes, 30 minutes, 1 hour, 4 hours, and 24 hours.

#### 2.4. Mix proportion and variations

The manufacture of test specimens was carried out based on the mortar mix design calculations and references from the literature [12] to obtain the optimal proportion. Variations were prepared by combining different proportions of pozzolanic material. In the mix design, the ratio between pozzolan and alkaline activator solution was set at 70%:30%, with the alkaline activator prepared at a ratio of 1:2.5 and a concentration of 12 molar. To improve workability, 2% superplasticizer (SP) and 5% additional water were incorporated into the mixture. The variations included rice husk ash at 0%, 6%, 9%, and 12% replacement levels, combined with *Bacillus subtilis* bacteria at concentrations of 0%, 0.5%, 1%, and 1.5%. The detailed mix design for 1 m<sup>3</sup> of mortar specimens is presented in Table 1, while the variations of test specimens are shown in Table 2.

**Table 1.** Mix proportion of the specimens for 1 m<sup>3</sup>

Sand (gram)	Pozzolan (gram)	NaOH (gram)	Na <sub>2</sub> SiO <sub>3</sub> (grams)	SP	Water Extra
1265	724.5	88.71	221.786	15	29

**Table 2.** Variation of test specimens

Variations	Pozzolan variations in weight
A	FA 100%
B	FA 100% + ASP 0% + BS 0%
C	FA 94% + ASP 6% + BS 0%
D	FA 91% + ASP 9% + BS 0%
E	FA 88% + ASP 12% + BS 0%
F	FA 99.5% + ASP 0% + BS 0.5%
G	FA 93.5% + ASP 6% + BS 0.5%
H	FA 90.5% + ASP 9% + BS 0.5%
I	FA 87.5% + ASP 12% + BS 0.5%
J	FA 99% + ASP 0% + BS 1%
K	FA 93% + ASP 6% + BS 1%

L	FA 90% + ASP 9% + BS 1%
M	FA 87% + ASP 12% + BS 1%
N	FA 98.5% + ASP 0% + BS 1.5%
O	FA 92.5% + ASP 6% + BS 1.5%
P	FA 89.5% + ASP 9% + BS 1.5%

Description:

FA : Fly Ash

ASP : Rice Husk Ash

BS. : *Bacillus Subtilis*

All mechanical and durability tests were conducted with replication and appropriate statistical treatment. For each mix variation and testing age, compressive strength tests were performed on  $n = 3$  specimens (three  $50 \times 50 \times 50$  mm cubes) and results are reported as mean  $\pm$  standard deviation (SD). For other tests (e.g., flexural / self-healing crack closure measurements, water absorption, and microstructural observations)  $n = 3$  replicates were used. Compressive strength was measured using  $50 \times 50 \times 50$  mm cubes in accordance with ASTM C109/C109M. Although structural concrete standards such as EN 12390 and EN 206 commonly use 150-mm cubes, these standards do not prescribe a universal conversion factor because size effects are highly mixture-dependent and smaller specimens often exhibit different strength behavior. Therefore, the measured values on 50-mm cubes are reported directly without applying an empirical correction to “equivalent” 150-mm cube strength, thereby avoiding additional uncertainty.

Control mixtures were prepared to establish baseline mechanical and durability performance. Two types of controls were included: (i) a cement-only control, produced using ordinary Portland cement without any geopolymer constituents, bacteria, or rice husk ash (RHA), and (ii) a geopolymer-only control, formulated using the same alkali-activated binder system but without bacterial culture or RHA incorporation. These controls enable direct comparison with the bio-modified geopolymer mixtures, isolating the effects of bacterial activity and RHA addition on strength development, patch repair behavior, and self-healing performance. The inclusion of both controls is essential to validate the experimental findings, ensuring that any observed enhancements can be attributed specifically to the bio-modification rather than to the underlying cementitious or geopolymer matrix.

### 3. Results and Discussion

#### 3.1. Materials characteristic

The fine aggregate test results indicated that the material met the requirements of the Indonesian National Standard (SNI). The fine aggregate exhibited a specific gravity of 2.50, a fineness modulus (MHB) of 2.71, a moisture content of 3.41%, and a mud content of 0.5%. These values confirm the suitability of the fine aggregate for use in the preparation of test specimens. The detailed results of the fine aggregate characteristics are presented in Table 3.

**Table 3.** Test results of fine aggregate (sand)

Testing Item	Results	Standard	Specifications
Specific gravity	2.50	2.5-2.7	SNI 1970:2016
Finess modulus	2.71	2.2-3.1	SNI ASTM C136-2012
Water Content	3.41%	3%-5%	SNI 1971:2011
Sludge Content	0.5%	<5%	SK SNI S-04-1989 F

The XRF (X-ray fluorescence) and FTIR (Fourier Transform Infrared Spectroscopy) analyses of rice husk ash indicated that silicon (Si) was the most dominant element, with a concentration of 14%. The high silica content confirms the potential of rice husk ash as a pozzolanic material suitable for application in bio-patch repair. The detailed XRF results are presented in Table 4, while the FTIR spectra are shown in Figure 1. Characterization of silica in rice husk ash using FTIR was conducted to identify the functional groups associated with Si-OH and Si-O-Si bonds. The IR spectrum, presented in Figure 1, illustrates the relationship between wave number and intensity. A distinct absorption peak was observed at  $1063\text{ cm}^{-1}$ , corresponding to the Si-O-Si siloxane functional group, confirming the presence of silica in the rice husk ash.

**Table 4.** Rice husk ash XRF test results

Pozzolan	Si	Al	Fe	Ca
Rice Husk Ash	63,43%	10,12%	15,39%	17,34%

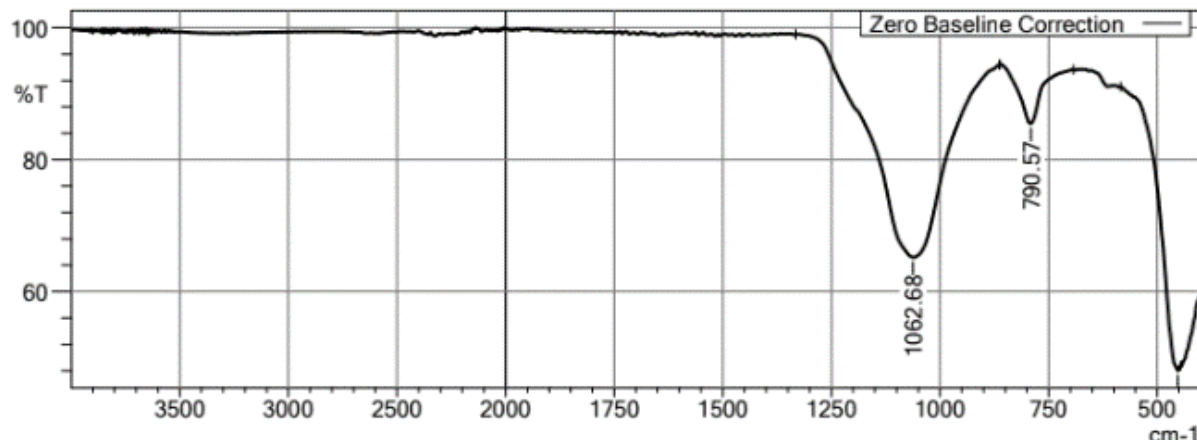


**Figure 1.** FTIR test results of rice husk ash

To ensure consistency with standard oxide-based reporting conventions, the elemental silica value obtained from the XRF test was converted to its oxide equivalent. The updated analysis shows that the RHA contains 63.43 wt% elemental Si, which corresponds to a substantially higher silica content than initially reported and reflects a more accurate representation of the material's chemical composition. Although this level remains lower than the 87–97 wt%  $\text{SiO}_2$  typically associated with high-purity pozzolanic RHA, it is characteristic of medium-grade ash influenced by combustion conditions, residual unburnt material, and naturally occurring mineral impurities. The presence of measurable quantities of Al, Fe, and Ca further supports this interpretation, indicating that the ash contributes both limited pozzolanic reactivity and micro-filler effects. Accordingly, the corrected oxide-based data provide a more robust basis for interpreting the RHA's role within the binder system and ensuring consistency with established materials-characterization standards.

The characterization of the bacteria confirmed that the identified strain was consistent with the descriptions reported in the literature [39–41] for application in concrete. The detailed results of bacterial characterization are presented in Table 5.

**Table 5.** Results of bacterial identification and characterization

Colony characterization	Cell characterization	Physiology
White Color	Bacil cell shape	Aerobic Aerobility

Myceloid colony shape	Gram-positive properties	Catalase Positive
Shape of erose edge		
Low convex elevation		
Structure in Opaque		

### 3.2. Fresh Materials Properties

The fresh properties of the materials were evaluated through flow table and density tests. The flow table test demonstrated that all variations satisfied the requirements of SNI 6882-2014, with flow values ranging from 105% to 115%. These results indicate that the bio-patch repair mortar exhibited adequate workability, ensuring ease of application in the field and the production of uniform, high-quality mixtures. The flow table test results are presented in Figure 2.

The density test, conducted in accordance with SNI 1973-2016, showed density values ranging from 2.27 to 2.40 g/cm<sup>3</sup> across all variations. The lowest density was recorded for variation D (88% FA + 12% RHA + 0% BS) at 2.27 g/cm<sup>3</sup>, while the highest density was obtained in variation N (92.5% FA + 6% RHA + 1.5% BS) at 2.40 g/cm<sup>3</sup>. These values fall within the range of 2.20–2.40 g/cm<sup>3</sup>, classified as normal concrete [13], confirming that the bio-patch repair mortar is suitable for general construction applications. The density test results are shown in Figure 3. All mix variations in this study were evaluated using three replicate specimens to ensure statistical reliability and to minimize the influence of sample-to-sample variability. The reported mechanical and durability performance values therefore represent the average of these three specimens, with the use of triplicate testing aligned with standard experimental practice in cementitious and geopolymers research.

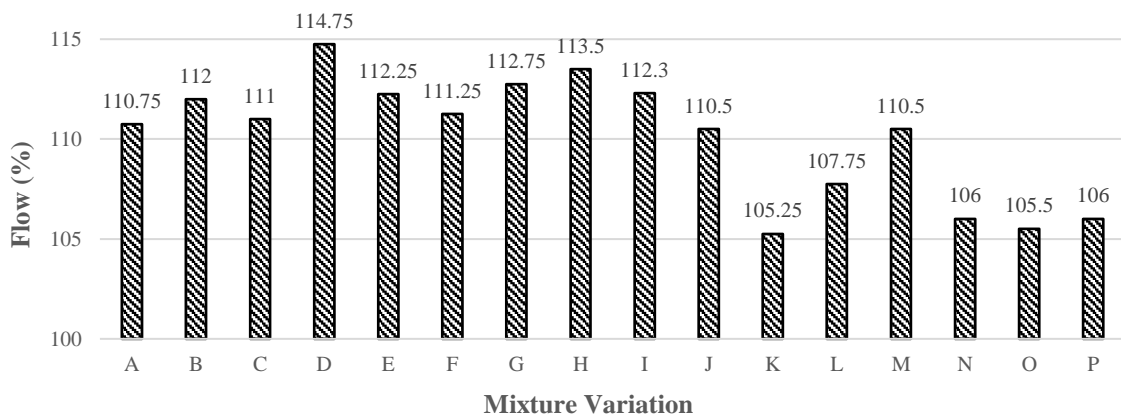


**Figure 2.** Flow table test results

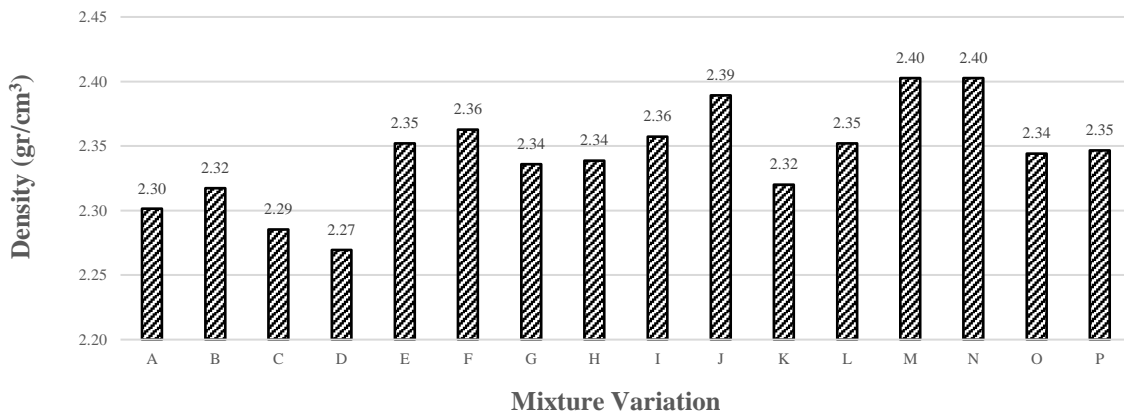


**Figure 3.** Density test results

### 3.3. Hardened Materials Properties

The hardened properties of the bio-patch repair mortar were evaluated through a series of tests, including compressive strength, shrinkage, and water absorption. The evaluation of hardened properties was likewise performed on three replicate specimens for each mix variation to ensure measurement accuracy and representativeness. All reported values for compressive strength, density, and other hardened-state parameters therefore reflect the mean of these three specimens, in accordance with standard practice for cementitious material characterization.

The compressive strength of the mortar at 28 days was determined using 5 cm cube specimens, and the values were subsequently converted to 15 cm cubes with a conversion factor of 0.8447. In accordance with SNI 03-2847-2002, the compressive strength of the 15 cm cube specimens was further converted to the equivalent value of a standard concrete cylinder specimen (15 cm in diameter and 30 cm in height) using a conversion factor of 0.83. The results, presented in Figure 4, demonstrate that the compressive strength development is strongly influenced by the chemical composition of the constituent materials.

Shrinkage performance was assessed after 28 days of curing, with a maximum permissible standard shrinkage of 0.10 cm. The highest shrinkage was observed in Variation A (FA100% + ASP0% + BS0%), with a value of 0.0233 cm, while the lowest shrinkage was recorded in Variation K (FA90% + ASP9% + BS1%) at 0.0011 cm. These results highlight the excellent dimensional stability of the bio-patch repair mortar, where low shrinkage minimizes the risk of cracking and enhances long-term durability.

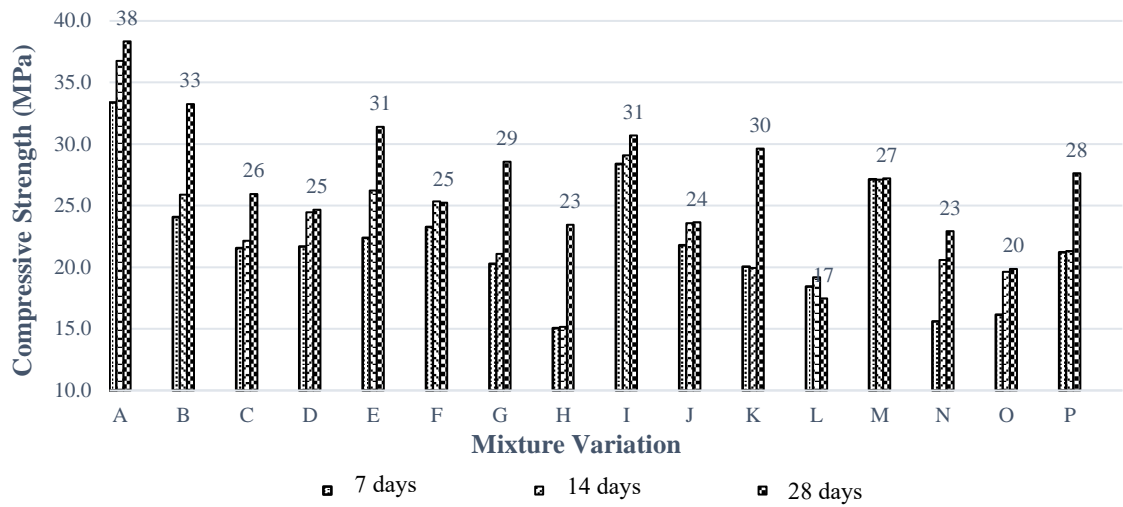


**Figure 4.** Compressive strength test results

The absorption test, carried out according to ASTM C1403-15, provided further insights into the durability characteristics of the mortar. All variations exhibited absorption values within the acceptable range of 2–7%. The highest absorption was obtained in Variation H (FA87% + ASP12% + BS1%), while the lowest was observed in Variation E (FA99% + ASP0% + BS1%). These findings indicate that the bio-patch repair mortar has low porosity, which contributes to improved durability and enhanced resistance to sulfate attack. The results of the absorption test are illustrated in Figure 5.

The observed reductions in water absorption and drying shrinkage can be mechanistically explained by the microstructural characteristics of the bio-enhanced geopolymers matrix. SEM analysis revealed denser gel formation and improved pore refinement in mixtures incorporating bacterial treatment, indicating the deposition of microbially induced calcium carbonate ( $\text{CaCO}_3$ ) within capillary voids. This mineral infilling reduces pore connectivity and increases tortuosity, thereby limiting moisture ingress and restraining volumetric changes associated with drying. Consequently, the lower absorption is a direct manifestation of reduced permeability, whereas the decrease in shrinkage reflects the diminished availability of free water and the stronger internal skeleton produced by the combined geopolymers gel and bacterially precipitated  $\text{CaCO}_3$ . This mechanistic linkage demonstrates that the improved durability indices are not merely empirical observations but arise from measurable microstructural modifications.

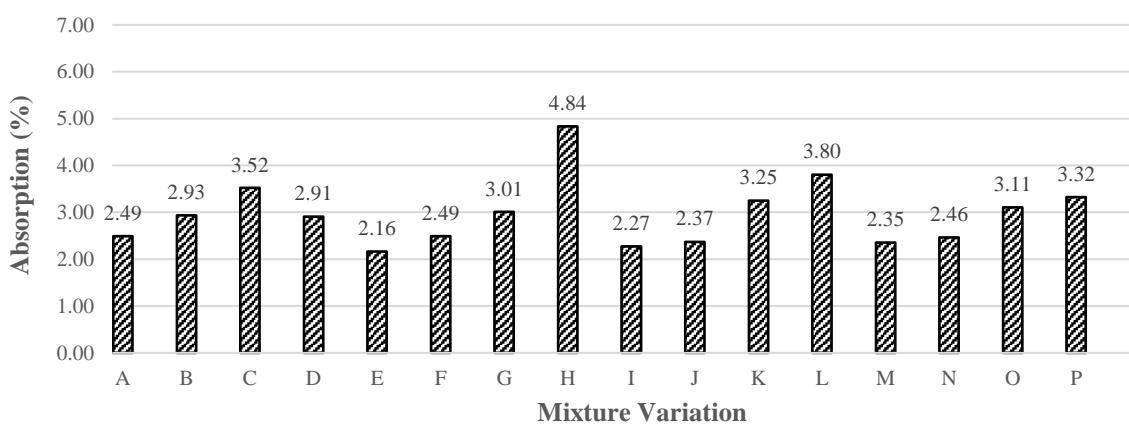


**Figure 5.** Absorption test results

The long-term viability of the incorporated bacteria is a critical factor influencing the sustained corrosion-inhibition capacity of the bio-geopolymer system. Although the geopolymer matrix exhibits a highly alkaline environment ( $\text{pH} > 12$ ), certain spore-forming bacteria such as *Bacillus* spp. are known to withstand extreme alkalinity by entering a dormant state, enabling them to remain viable until reactivated by moisture ingress or cracking. The protective mechanism therefore does not rely on continuous metabolic activity but on the ability of dormant spores to become active when microcracks or localized moisture appear, conditions that typically precede reinforcement corrosion. Upon reactivation, the bacteria precipitate  $\text{CaCO}_3$ , which seals microcracks, reduces oxygen and ion transport, and stabilizes the interfacial transition zone around steel reinforcement. This periodic self-healing response enhances the long-term durability of the matrix and contributes to extended corrosion protection beyond the initial curing period. Nevertheless, the longevity of bacterial functionality is influenced by pore solution chemistry, moisture cycling, and nutrient availability, and is addressed in this study through encapsulation strategies and optimized activator–nutrient balance.

#### 4. Conclusion

The bio-patch repair mortar demonstrated promising performance in both fresh and hardened states. The mixture exhibited good flowability and density within the range of normal concrete, ensuring ease of application and suitability for general construction. In hardened properties, the mortar achieved a compressive strength greater than 25 MPa at 28 days, fulfilling the requirements for patch repair applications. Additionally, the low shrinkage values confirmed its excellent dimensional stability, while the low absorption indicated reduced porosity and high durability. Collectively, these findings suggest that the bio-patch repair mortar offers reliable mechanical performance and durability, making it a viable and sustainable material for concrete repair.

#### Acknowledgements

The authors would like to express their sincere gratitude to Universitas Muhammadiyah Yogyakarta for the financial support provided throughout the research and publication process.

#### References

- [1] Wang H, Jiang M, Hang M, Yang Y, Zhou X, Liu X, et al. Inhibition resistance and mechanism of migrating corrosion inhibitor on reinforced concrete under coupled carbonation and chloride attack. *Journal of Building Engineering* 2023;76:107398. <https://doi.org/10.1016/J.JBEME.2023.107398>.
- [2] Astuti P, Rafdin RS, Yamamoto D, Hamada H. Natural Localized Corrosion of Steel Bar in 44-Years Old Cracked RC Beam Structures Exposed to Marine Tidal Environment, 2024, p. 371–81. [https://doi.org/10.1007/978-981-99-6018-7\\_27](https://doi.org/10.1007/978-981-99-6018-7_27).
- [3] Korec E, Jirásek M, Wong HS, Martínez-Pañeda E. Phase-field chemo-mechanical modelling of corrosion-induced cracking in reinforced concrete subjected to non-uniform chloride-induced corrosion. *Theoretical and Applied Fracture Mechanics* 2024;129:104233. <https://doi.org/10.1016/J.TAFMEC.2023.104233>.
- [4] Peng L, Zeng W, Zhao Y, Li L, Poon C sun, Zheng H. Steel corrosion and corrosion-induced cracking in reinforced concrete with carbonated recycled aggregate. *Cem Concr Compos* 2022;133:104694. <https://doi.org/10.1016/J.CEMCONCOMP.2022.104694>.
- [5] Luan H, Fan Y, Zhao L, Ju X, Shah SP. Corrosion characteristics and critical corrosion depth model of reinforcement at concrete cover cracking in an electrochemical accelerated corrosion environment. *Case Studies in Construction Materials* 2025;22:e04628. <https://doi.org/10.1016/j.cscm.2025.e04628>.
- [6] Ortolan TLP, Borges PM, Silvestro L, da Silva SR, Possan E, Andrade JJ de O. Durability of concrete incorporating recycled coarse aggregates: carbonation and service life prediction under

chloride-induced corrosion. Constr Build Mater 2023;404:133267. <https://doi.org/10.1016/J.CONBUILDMAT.2023.133267>.

[7] Amorim Júnior NS, Andrade Neto JS, Santana HA, Cilla MS, Ribeiro D V. Durability and service life analysis of metakaolin-based geopolymers concretes with respect to chloride penetration using chloride migration test and corrosion potential. Constr Build Mater 2021;287:122970. <https://doi.org/10.1016/j.conbuildmat.2021.122970>.

[8] Astuti P, Sasmita D, Isnaini MS, Zulkarnain A, Purnama AY, Monika F, et al. Assessing the Strength Characteristics and Environmental Impact of Fly-Ash Geopolymer Mortar for Sustainable Green Patch Repair: A Pathway towards SDGs Achievement. E3S Web of Conferences 2024;594:06001. <https://doi.org/10.1051/e3sconf/202459406001>.

[9] Kawai K, Nishida T, Saito A, Hayashi T. Application of bio-based materials to crack and patch repair methods in concrete. Constr Build Mater 2022;340:127718. <https://doi.org/10.1016/J.CONBUILDMAT.2022.127718>.

[10] Astuti P. The mechanical performance evaluation of fly-ash derived geopolymers mortar for concrete patch repair. Multidisciplinary Science Journal 2024;7:2025161. <https://doi.org/10.31893/multiscience.2025161>.

[11] Lu X, Liu B, Zhang Q, Wang S, Liu J, Li Q, et al. Mechanical properties and hydration of fly ash-based geopolymers modified by copper slag. Mater Today Commun 2024;39:108914. <https://doi.org/10.1016/J.MTCOMM.2024.108914>.

[12] Xu X, Bao S, Zhang Y, Ping Y. Sustainable enhancement of fly ash-based geopolymers: Impact of Alkali thermal activation and particle size on green production. Process Safety and Environmental Protection 2024;191:478–89. <https://doi.org/10.1016/J.PSEP.2024.08.133>.

[13] Astuti P, Afriansya R, Anisa EA, Randisyah J. Mechanical properties of self-compacting geopolymers concrete utilizing fly ash, 2022, p. 020028. <https://doi.org/10.1063/5.0094463>.

[14] Afriansya R, Astuti P, Ratnadewati VS, Randisyah J, Ramadhona TY, Anisa EA. Investigation of setting time and flowability of geopolymers mortar using local industry and agriculture waste as precursor in Indonesia. International Journal of GEOMATE 2021;21. <https://doi.org/10.21660/2021.87.j2325>.

[15] Afriansya R, Anisa EA, Astuti P, Cahyati MD. Effect of polypropylene fiber on workability and strength of fly ash-based geopolymers mortar. E3S Web of Conferences 2023;429:05006. <https://doi.org/10.1051/e3sconf/202342905006>.

[16] Zia ul haq Md, Sood H, Kumar R, Chandra Jena P, Kumar Joshi S. Eco-friendly approach to construction: Incorporating waste plastic in geopolymers concrete. Mater Today Proc 2023. <https://doi.org/10.1016/j.matpr.2023.09.037>.

[17] Khalaf AA, Kopecskó K, Modhfar S. Applicability of waste foundry sand stabilization by fly ash geopolymers under ambient curing conditions. Heliyon 2024;10:e27784. <https://doi.org/10.1016/J.HELION.2024.E27784>.

[18] Wang X, Cheng C, Wang D. Effect of rice husk ash on mechanical properties of rubber doped geopolymers recycled concrete. Case Studies in Construction Materials 2024;20:e03406. <https://doi.org/10.1016/J.CSCM.2024.E03406>.

[19] Kumar S, Sekhar Das C, Lao J, Alrefaei Y, Dai JG. Effect of sand content on bond performance of engineered geopolymers composites (EGC) repair material. Constr Build Mater 2022;328:127080. <https://doi.org/10.1016/J.CONBUILDMAT.2022.127080>.

[20] Yang L, Zhu Z, Sun H, Huo W, Zhang J, Wan Y, et al. Durability of waste concrete powder-based geopolymers reclaimed concrete under carbonization and freeze–thaw cycles. Constr Build Mater 2023;403:133155. <https://doi.org/10.1016/j.conbuildmat.2023.133155>.

[21] Wudil YS, Al-Fakih A, Al-Osta MA, Gondal MA. Intelligent optimization for modeling carbon dioxide footprint in fly ash geopolymers concrete: A novel approach for minimizing CO<sub>2</sub> emissions. J Environ Chem Eng 2024;12:111835. <https://doi.org/10.1016/j.jece.2023.111835>.

[22] Al-Shaeer HAY, Alshalif AF, Amran M, Gushgari SY, Irwa JM, Mansour MA, et al. Innovative development of bio-foam concrete using rice husk ash, eggshell powder, and *Bacillus tequilensis*:

Mechanical, durability, and microstructural performance. *Journal of Building Engineering* 2025;113:113934. <https://doi.org/10.1016/j.jobe.2025.113934>.

[23] Ahmad SSE, Elshazly MA, Elakhras AA, Elshami AA, Elmahdy MAR, Aboubakr A. Thermal dependency of microbial self-healing of concrete: Comparing the effectiveness of *Bacillus* strains at different temperatures, from room temperature to below zero. *Case Studies in Construction Materials* 2025;23:e05182. <https://doi.org/10.1016/j.cscm.2025.e05182>.

[24] Ul Islam S, Waseem SA. Strength retrieval and microstructural characterization of *Bacillus subtilis* and *Bacillus megaterium* incorporated plain and reinforced concrete. *Constr Build Mater* 2023;404:133331. <https://doi.org/10.1016/j.conbuildmat.2023.133331>.

[25] Tie Y, Ji Y, Zhang H, Jing B, Zeng X, Yang P. Investigation on the mechanical properties of *Bacillus subtilis* self-healing concrete. *Helion* 2024;10:e34131. <https://doi.org/10.1016/j.heliyon.2024.e34131>.

[26] Nindhita KW, Zaki A, Zaini M, Kusumawijaya AM. Corrosion analysis of concrete based on industrial waste and bacteria by non-destructive test methods. *Scientific Review Engineering and Environmental Sciences (SREES)* 2025;34:109–27. <https://doi.org/10.22630/srees.10299>.

[27] Nindhita KW, Zaki A, Zeyad AM. Effect of *Bacillus Subtilis* Bacteria on The Mechanical Properties of Corroded Self-Healing Concrete. *Frattura Ed Integrità Strutturale* 2024;18:140–58. <https://doi.org/10.3221/IGF-ESIS.68.09>.

[28] Feng S, Ge C, Sun Q, Zheng W, Li G, Hu C. Valorization of agriculture waste: Preparation of alkoxysilanes from mixed rice straw and rice husk ash. *Chemical Engineering Journal* 2024;495:153377. <https://doi.org/10.1016/J.CEJ.2024.153377>.

[29] Hirose Carlsen MM, Saito Y. Phase diagram of  $\text{SiO}_2$  crystallization upon rice husk combustion to control silica ash quality. *Waste Management* 2024;182:55–62. <https://doi.org/10.1016/J.WASMAN.2024.04.009>.

[30] Astuti P, Afriansya R, Anisa EA, Puspitasari SD, Purnama AY. The potential use of agriculture pozzolan waste as supplementary cementitious materials by integrating with biomass, 2022, p. 040017. <https://doi.org/10.1063/5.0104926>.

[31] Alrowaili ZA, Alnairi MM, Olarinoye IO, Alhamazani A, Alshammari GS, Al-Buriahi MS. Radiation attenuation of fly ash and rice husk ash-based geopolymers as cement replacement in concrete for shielding applications. *Radiation Physics and Chemistry* 2024;217:111489. <https://doi.org/10.1016/J.RADPHYSCHED.2023.111489>.

[32] Kaze RC, Naghizadeh A, Tchadjie L, Cengiz Ö, Kamseu E, Chinje FU. Formulation of geopolymer binder based on volcanic-scoria and clay brick wastes using rice husk ash-NaOH activator: Fresh and hardened properties. *Sustain Chem Pharm* 2024;40:101627. <https://doi.org/10.1016/J.JSCP.2024.101627>.

[33] Hou Y, Yang K, Yin S, Yu X, Wang L, Yang X. Enhancing the physical properties of cemented ultrafine tailings backfill (CUTB) with fiber and rice husk ash: Performance, mechanisms, and optimization. *Journal of Materials Research and Technology* 2024;29:4418–32. <https://doi.org/10.1016/J.JMRT.2024.02.068>.

[34] Nanda B, Mishra J, Patro SK. Synthesis of rice husk ash based alkaline activators for geopolymer binder systems: A review. *Journal of Building Engineering* 2024;91:109694. <https://doi.org/10.1016/J.JOBE.2024.109694>.

[35] Chelluri SK, Hossiney N. Performance evaluation of ternary blended geopolymer binders comprising of slag, fly ash and brick kiln rice husk ash. *Case Studies in Construction Materials* 2024;20:e02918. <https://doi.org/10.1016/J.CSCM.2024.E02918>.

[36] Narattha C, Wattanasiriwech S, Wattanasiriwech D. Sustainable, multifunctional fly ash geopolymer composite with rice husk aggregates for improved acoustic, hygric, and thermal performance. *Constr Build Mater* 2024;445:137743. <https://doi.org/10.1016/J.CONBUILDMAT.2024.137743>.

[37] Gandhi H, Beladiya U, Poriya M, Vaghela J, Mevada V, Patel R, et al. Carbon capture and sequestration through landfill-derived *Bacillus* strains: Enhanced microbially induced calcite

precipitation for sustainable bio-brick production. *Constr Build Mater* 2025;491:142600. <https://doi.org/10.1016/j.conbuildmat.2025.142600>.

[38] Hajee I, Harrison STL, Kotsopoulos A. Microbially-induced calcite precipitation in heterogeneous co-disposed coal waste systems. *Miner Eng* 2025;232:109530. <https://doi.org/10.1016/j.mineng.2025.109530>.

[39] Abu Bakr M, Singh BK, Deifalla AF, Pandey S, Hussain A, Ragab AE, et al. Assessment of the mechanical and durability characteristics of bio-mineralized *Bacillus subtilis* self-healing concrete blended with hydrated lime and brick powder. *Case Studies in Construction Materials* 2023;19:e02672. <https://doi.org/10.1016/j.cscm.2023.e02672>.

[40] Cahyati MD, Huang W-H, Hsu H-L, Winata C. Self-healing investigation on engineered cementitious composites incorporating *Bacillus subtilis* immobilized in silica gel. *Case Studies in Construction Materials* 2025;23:e05130. <https://doi.org/10.1016/j.cscm.2025.e05130>.

[41] Premalatha PV, Geethanjali M, Sundararaman S, Murali CS. An experimental investigation on self-healing concrete using “*Bacillus subtilis*.” *Mater Today Proc* 2023. <https://doi.org/10.1016/j.matpr.2023.08.118>.